

## Entropy Analysis of Nanofluid flow in a Fluidized Bed Dryer in Presence of Induced Magnetic Field

Kiptum J. Purity<sup>1,\*</sup>, Mathew N. Kinyanjui<sup>2</sup>, Edward R. Onyango<sup>2</sup>

<sup>1</sup>*Pan African University Institute for Basic Sciences, Technology and Innovation, Nairobi, Kenya*

<sup>2</sup>*Department of Pure and Applied Mathematics, Jomo Kenyatta University of Agriculture and Technology, Nairobi, Kenya*

\*Corresponding author: pkiptum@gmail.com

**Abstract.** The study investigates generation of entropy in an unsteady, incompressible nanofluid flow occurring within a fluidized bed dryer used in tea processing industries. The study considered the presence of variable magnetic field, influence of viscous dissipation, thermal radiation and chemical reaction. The nonlinear partial differential equations of momentum, energy and concentration were derived. A finite difference numerical scheme was employed to obtain an approximate solution for the nonlinear partial differential equations governing the flow. Entropy generation is then determined from velocity, concentration and temperature profiles obtained from solution of momentum, mass and energy equations. The study illustrated the impact of various flow parameters on entropy generation and Bejan number through graphical presentations while numerical values for skin friction coefficient, heat and mass transfer rates were provided in tabular form. Study of entropy generation allows one identify factors which contribute to energy inefficiencies in a thermal system and allows different stakeholders or designers of bed dryers in tea factories identify ways of improving the dryer or designing more effective dryers. Bejan number is used in thermodynamics to evaluate efficiency of thermal systems such as fluidized bed dryers. It helps one design heat exchangers which maximizes heat transfer while minimizing energy losses. The findings of this study are essential in improving the performance, efficiency and the design of a fluidized bed dryer involving heat and mass transfer as well as fluid flow.

### LIST OF SYMBOLS

- $(v_r, v_z)$  - Velocity components
- $T_\infty$  - Free stream temperature (K)
- $T_b$  - Temperature at the dryer's bed (K)
- $C_b$  - Concentration at the dryer's bed ( $\text{Mol } m^{-3}$ )
- $H_0$  - Applied magnetic field ( $Wbm^{-2}$ )
- $P$  - Pressure ( $Nm^{-2}$ )
- $F_b$  - Buoyancy force (N)
- $g$  - acceleration due to gravity ( $ms^{-2}$ )
- $k_s$  - Solid fraction thermal conductivity (W/m.K)
- $k_{nf}$  - Nanofluid thermal conductivity (W/m.K)
- $D_{nf}$  - Diffusion coefficient ( $m^2s^{-1}$ )
- $g_z$  - gravitational force along z direction ( $ms^{-2}$ )

Received: Oct. 13, 2023.

2020 *Mathematics Subject Classification.* 35Q79.

*Key words and phrases.* entropy; Bejan number; heat transfer; mass transfer; nanofluid; fluidized bed dryer.

- $F_{EM}$  - Lorentz force (N)
- $Q^*$  - Heat source (J)
- $k_r$  - Chemical reaction parameter
- $U, V$  - Dimensionless velocity
- $Re$  - Reynolds number
- $Gr_T$  - Thermal Grashof number
- $Gr_C$  - Concentration Grashof number
- $Ec$  - Eckert number
- $M$  Hartmann number
- $Pr$  - Prandtl number
- $Sc$  - Schmidt number
- $\mu_{nf}$  - Dynamic viscosity of nanofluid ( $kgm^{-1}s^{-1}$ )
- $\rho_{nf}$  - Nanofluid density ( $kg^{-3}$ )
- $(\rho C_p)_{nf}$  - Nanofluid heat capacitance (J/K)
- $\sigma_{nf}$  - Electrical conductivity ( $\omega^{-1}m^{-1}$ )

## 1. INTRODUCTION

The process of tea production involves the following stages: harvesting, withering, rolling, oxidation, drying and sorting. Tea drying is one of the energy intensive processes in tea manufacturing and many tea processing industries in most countries in the world depend on different methods to dry their tea. Use of fluidized bed dryers is one of the most efficient methods utilized in this process. The primary method of heat transfer in a fluidized bed dryer is convection.

Entropy generation is a thermodynamic quantity which represents unavailability of system's thermal energy or conversion into mechanical work. Entropy is the level of randomness or disorder in the system as the amount of available energy for use is lost. In relation to fluidized bed dryer, entropy generation occurs due to heat transfer inefficiencies and other dissipative processes. The concept of entropy was introduced by Clausius [1] from 1850-1864 on the theory of heat and its applications related to engines. Bejan [2, 3, 4] introduced several factors responsible for entropy generation in thermal systems. These include heat transfer, mass transfer, viscous dissipation, chemical reaction and electrical conduction. Bejan [5], studied entropy generation minimization in a thermodynamic system so as to improve its thermal efficiency.

High production of entropy can lead to energy inefficiencies, longer drying time and reduced tea quality. Therefore, efforts need to be put in place to minimize production of entropy by adopting energy efficient methods, industry operational practices as well as improving dryers' design so as to optimize the drying process in the tea manufacturing. Efficiency and sustainability in energy systems are becoming increasingly important, and this requires taking into account the limitations set by the second law of thermodynamics. One method for achieving this is by using entropy generation analysis, which is more effective than traditional energy balance approaches. It can identify the sources of inefficiency and aid in designing more efficient systems. Additionally, because it is based on basic thermodynamic principles, it can be used for any type of energy conversion system. This has made entropy generation analysis a widely used method in the design and optimization of sustainable energy systems. Many researchers have investigated entropy generation in flows, which is crucial in engineering systems, by examining different fluid flow scenarios, boundary conditions, and geometric configurations.

Bulgakov et al.[6] designed an efficient dryer with an aim of optimizing the drying process by introducing the concept of vibro-boiling conditions. These conditions were achieved through vertical oscillations of the dryer's body. Vibro boiling conditions led to better heat transfer and

reduced temperature gradients which lead to lower entropy production. With the use of a mathematical model, they were able to predict and optimize parameters such as heat transfer area and heat transfer coefficient which ensured that the drying process was as efficient as possible. Inaba et al. [7] explored entropy reduction by optimizing heat and mass transfer in fluidized bed dryer by considering influence of parameters such as moisture content, air temperature and Reynolds number. The research noted that energy and exergy efficiencies decreased as moisture content; thus low moisture content reduced entropy production. It was also found that low Reynolds number enhanced the drying process i.e. reducing the fluid's motion contributed to entropy reduction. Increase in fluid's temperature contributed to reduced entropy, however, high temperatures was noted to damage the material. Deymi-Dashtebayaz [8] examined a fluidized bed dryer at Jovein citric acid Production Company in Iran to study its energy and exergy performance. To improve exergy and energy efficiencies within the dryer, they adopted several strategies. These include lowering the air flow rate and air temperature which led to decrease of energy required during the drying process. This resulted in reduced energy loss hence low entropy production. Others include reducing moisture content of the final product and reducing heat losses from the dryer. The study carried out by Razavikia et al. [9] emphasized the importance of thermodynamic analysis as a tool used for analyzing and designing optimal thermal systems including the fluidized bed dryers. The study noted that fluidized bed dryers are used in various industrial applications although it is associated with high energy consumption. By developing a thermodynamic model for drying processes, they applied the simultaneous equations for mass and heat transfer processes to analyse the thermodynamic processes in a fluidized bed dryer. The study took into consideration various parameters such as inlet air temperature, air humidity, difference input and output of products and air humidity ratio. The researchers noted that model developed could be used to optimize the drying process as well as assist researchers and engineers assess the thermal efficiency and losses during the energy conversion processes.

Nanoparticles were first initiated by Choi et al. [10] to investigate thermal conductivity and thermophysical property effectiveness of base fluids (water, ethylene glycol and oil) by adding nanoparticles. Hence addition of nanoparticles to base fluid has been found to enhance thermal conductivity, a parameter responsible for heat transfer. Fluid flow in presence of magnetic field is known as hydromagnetic. Jerry et al. [11] showed that heat transfer with nanoparticles in hydromagnetic flow affects entropy generation .

Tea drying being an irreversible process, involves chemical and physical changes which can affect quality of the final product. During fluidization some energy which could have been fully transformed to useful work is lost through dissipation or thermal radiation. Given importance of energy costs, fuel availability and environmental impact, studying of entropy generation is important to enable tea processing factories not only save energy but also use it efficiently.

The primary motivation for this research stems from the limited available literature on entropy generation of fluidized bed dryers which takes into consideration nanoparticles and the influence

of variable magnetic field during the heat and mass transfer processes. Thus the aim of this study is to explore entropy generation within a FBD of an incompressible nanofluid flow. The research takes into account the effects of viscous dissipation and thermal radiation. To achieve this, numerical computations are carried out by use of finite difference method, including various values of pertinent parameters. This paper therefore, explores entropy generation of a nanofluid flow within a fluidized bed dryer as well as the dynamics of heat and mass transfer processes. The findings are presented through a combination of tabular and graphical representations.

## 2. MATHEMATICAL FORMULATION

Consider a two dimensional nanofluid flow within a fluidized bed dryer. In this configuration, the  $z$ -axis aligns with the dryer's axis while  $r$ -axis is along the radial direction as shown in figure 1. A uniform magnetic field of strength  $B_0$  is applied in the radial direction leading to generation of induced magnetic field  $B = (B_r, 0, B_z)$  in axial direction. The lower part of the dryer is heated by convection from hot air at temperature  $T_b$  while ambient temperature is  $T_\infty$  where  $T_b > T_\infty$ .

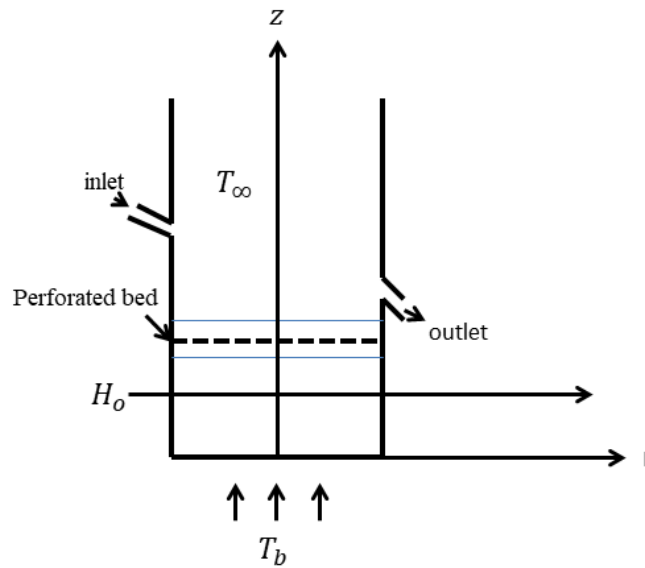


FIGURE 1. Geometry of the problem

The nonlinear partial differential equations that describe the fluid flow within the fluidized bed dryer in presence of variable magnetic field are expressed as follows:

$$\frac{1}{r} \frac{\partial(rv_r)}{\partial r} + \frac{\partial v_z}{\partial z} = 0 \quad (2.1)$$

$$\rho_{nf} \left( \frac{\partial v_r}{\partial t} + v_r \frac{\partial v_r}{\partial r} + v_z \frac{\partial v_r}{\partial z} \right) = -\frac{\partial P}{\partial r} + \mu_{nf} \left( \frac{\partial^2 v_r}{\partial r^2} + \frac{1}{r} \frac{\partial v_r}{\partial r} + \frac{\partial^2 v_r}{\partial z^2} - \frac{v_r}{r^2} \right) + \sigma_{nf} \mu_e^2 \left( v_z (H_r H_z + H_0 H_z) - v_r H_z^2 \right) \quad (2.2)$$

$$\rho_{nf} \left( \frac{\partial v_z}{\partial t} + v_r \frac{\partial v_z}{\partial r} + v_z \frac{\partial v_z}{\partial z} \right) = \mu_{nf} \left( \frac{\partial^2 v_z}{\partial r^2} + \frac{1}{r} \frac{\partial v_z}{\partial r} + \frac{\partial^2 v_z}{\partial z^2} \right) - \mathbf{g} \rho_{nf} \left( \beta_{Tnf} (T_b - T_\infty) + \beta_{Cnf} (C_b - C_\infty) \right) + \sigma_{nf} \mu_e^2 \left( v_r (H_0 H_z + H_z H_r) - v_z (H_r^2 + 2H_0 H_r + H_0^2) \right) \quad (2.3)$$

$$(\rho C_p)_{nf} \left( \frac{\partial T}{\partial t} + v_r \frac{\partial T}{\partial r} + v_z \frac{\partial T}{\partial z} \right) = k_{nf} \left[ \frac{1}{r} \frac{\partial}{\partial r} \left( r \frac{\partial T}{\partial r} \right) + \frac{\partial^2 T}{\partial z^2} \right] + \mu_{nf} \left( 2 \left[ \left( \frac{\partial v_r}{\partial r} \right)^2 + \left( \frac{\partial v_z}{\partial z} \right)^2 \right] + \left( \frac{\partial v_r}{\partial z} + \frac{\partial v_z}{\partial r} \right)^2 \right) - \frac{16\sigma^*}{3k^*} T_\infty^3 \frac{\partial T}{\partial r} + Q^* (T_b - T_\infty) \quad (2.4)$$

$$\frac{\partial C}{\partial t} + v_r \frac{\partial C}{\partial r} + v_z \frac{\partial C}{\partial z} = D_{nf} \left( \frac{\partial^2 C}{\partial r^2} + \frac{\partial^2 C}{\partial z^2} \right) - k_r (C_\infty - C_b) \quad (2.5)$$

subject to

$$\begin{aligned} t \geq 0 : r = 0 : v_r = 0, v_z = U, T = T_\infty, C = C_\infty, H_r = 0, H_z = H_0 \\ r_{\text{wall}} = R : v_r = 0, v_z = 0, T = T_b, C = C_b, T_\infty > T_b, C_\infty < C_b, H_r = 0, H_z = 0 \\ z = 0 : T = T_b, C = C_b, v_z = 0, H_r = 0, H_z = 0 \\ z = z_{\text{max}} : T = T_\infty, C = C_\infty, v_z \rightarrow v_\infty = 0, H_r = 0, H_z = 0 \end{aligned} \quad (2.6)$$

Referring to Das et al. [12], Mehta et al. [13], the expressions for thermophysical properties of nanofluid dynamic viscosity, density, thermal expansion coefficient, heat capacitance, effective thermal conductivity and electrical conductivity are given by

$$\mu_{nf} = \frac{\mu_f}{(1 - \phi)^{2.5}}$$

$$\rho_{nf} = (1 - \phi)\rho_f + \phi\rho_s$$

$$\beta_{nf} = (1 - \phi)\beta_f + \phi\beta_s$$

$$(\rho C_p)_{nf} = (1 - \phi)(\rho C_p)_f + \phi(\rho C_p)_s$$

$$\frac{k_{nf}}{k_f} = \frac{(k_s + 2k_f) - 2\phi(k_f - k_s)}{(k_s + 2k_f) + \phi(k_f - k_s)}$$

$$\sigma_{nf} = (1 - \phi)\sigma_f + \phi\sigma_s$$

The following transformational variables are used to convert equations (2.2), (2.3), (2.4) and (2.5) in dimensionless form.

$$\begin{aligned} v_r^* = \frac{v_r}{U}, v_z^* = \frac{v_z}{U}, r^* = \frac{r}{R}, P^* = \frac{P}{\rho U^2}, t^* = \frac{Ut}{R}, z^* = \frac{z}{R}, T^* = \frac{T - T_\infty}{T_b - T_\infty} \\ C^* = \frac{C - C_\infty}{C_b - C_\infty}, H_z^* = \frac{H_z}{H_0}, H_r^* = \frac{H_r}{H_0} \end{aligned} \quad (2.7)$$

In non-dimensionalized form, equations (2.2), (2.3), (2.4) and (2.5) result in the following set of equations

$$\begin{aligned} \frac{\partial v_r^*}{\partial t^*} + v_r^* \frac{\partial v_r^*}{\partial r^*} + v_z^* \frac{\partial v_r^*}{\partial z^*} = -\frac{\partial P^*}{\partial r^*} + \frac{\phi_1}{\text{Re}} \left( \frac{\partial^2 v_r^*}{\partial r^{*2}} + \frac{1}{r^*} \frac{\partial v_r^*}{\partial r^*} - \frac{v_r^*}{r^{*2}} + \frac{\partial^2 v_r^*}{\partial z^{*2}} \right) \\ + \phi_2 \frac{M}{\text{Re}} \left( v_z^* (H_z^* (H_r^* + 1)) - v_r^* H_z^{*2} \right) \end{aligned} \quad (2.8)$$

$$\begin{aligned} \frac{\partial v_z^*}{\partial t^*} + v_r^* \frac{\partial v_z^*}{\partial r^*} + v_z^* \frac{\partial v_z^*}{\partial z^*} = \frac{\phi_1}{\text{Re}} \left( \frac{\partial^2 v_z^*}{\partial r^{*2}} + \frac{1}{r^*} \frac{\partial v_z^*}{\partial r^*} + \frac{\partial^2 v_z^*}{\partial z^{*2}} \right) - \phi_3 G_{rT} - \phi_3 G_{rC} \\ + \phi_2 \frac{M}{\text{Re}} \left( (v_r^* (H_z^* (1 + H_r^*))) - v_z^* (H_r^{*2} + 2H_r^* + 1) \right) \end{aligned} \quad (2.9)$$

$$\begin{aligned} \frac{\partial T^*}{\partial t^*} + v_r^* \frac{\partial T^*}{\partial r^*} + v_z^* \frac{\partial T^*}{\partial z^*} = \phi_4 \frac{1}{\text{Pr}} \frac{1}{\text{Re}} \left[ \frac{1}{r^*} \frac{\partial}{\partial r^*} \left( r^* \frac{\partial T^*}{\partial r^*} \right) + \frac{\partial^2 T^*}{\partial z^{*2}} \right] + \\ \phi_5 \frac{\text{Ec}}{\text{Re}} \left( 2 \left[ \left( \frac{\partial v_r^*}{\partial r^*} \right)^2 + \left( \frac{\partial v_z^*}{\partial z^*} \right)^2 \right] + \left( \frac{\partial v_r^*}{\partial z^*} + \frac{\partial v_z^*}{\partial r^*} \right)^2 \right) - \\ \phi_6 \frac{q_r}{\text{PrRe}} + \phi_6 \Omega \end{aligned} \quad (2.10)$$

$$\frac{\partial C^*}{\partial t^*} + v_r^* \frac{\partial C^*}{\partial r^*} + v_z^* \frac{\partial C^*}{\partial z^*} = \frac{1}{\text{Sc}} \frac{1}{\text{Re}} \left( \frac{\partial^2 C^*}{\partial r^{*2}} + \frac{\partial^2 C^*}{\partial z^{*2}} \right) - K_1 \quad (2.11)$$

with dimensionless initial and boundary conditions as

$$\begin{aligned} t \geq 0 : r^* = 0 : v_r^* = 1, v_z^* = 1, T^* = 0, C^* = 0, H_r^* = 0, H_z^* = 1 \\ r_{\text{wall}}^* = 1 : v_r^* = 0, v_z^* = 0, T^* = 1, C^* = 1, H_r^* = 0, H_z^* = 0 \\ z = 0 : T^* = 1, C^* = 1, v_z^* = 0, H_r^* = 0, H_z^* = 0 \\ z = z_{\text{max}} : T^* = 0, C^* = 0, v_z^* = 0, H_r^* = 0, H_z^* = 0 \end{aligned} \quad (2.12)$$

where

$$\begin{aligned} \text{Re} = UR \frac{\rho_f}{\mu_f}, M = \frac{H_0^2 \mu_e^2 \sigma R^2}{\nu \rho}, G_{rT} = \frac{R \mathbf{g} \beta_{Tf} (T_b - T_\infty)}{U^2}, P^* = \frac{P}{\rho U^2}, \Omega = \frac{Q^*}{U(\rho C_p)_f}, K_1 = k_r \frac{R}{U} \\ t^* = \frac{Ut}{R}, z^* = \frac{z}{R}, T^* = \frac{T - T_\infty}{T_b - T_\infty}, G_{rC} = \frac{R \mathbf{g} \beta_{Cf} (C_b - C_\infty)}{U^2}, \text{Pr} = \frac{\nu(\rho C_p)_f}{k_f} \\ C^* = \frac{C - C_\infty}{C_b - C_\infty}, H_z^* = \frac{H_z}{H_0}, H_r^* = \frac{H_r}{H_0}, \text{Ec} = \frac{U^2}{C_{pf}(T_b - T_\infty)}, \text{Sc} = \frac{\nu}{D_{nf}} \end{aligned} \quad (2.13)$$

### 3. NUSSELT NUMBER, SHERWOOD NUMBER AND LOCAL SKIN FRICTION COEFFICIENT

Nusselt and Sherwood numbers are used to determine the rate of heat and mass transfer from the temperature and concentration profiles respectively. Nusselt number is given by

$$Nu = \frac{Rq_w}{k_f(T_b - T_\infty)} \quad (3.1)$$

where

$$q_w = -k_{nf} \left( 1 + \frac{16\sigma^* T_\infty^3}{3k^*} \right) \left( \frac{\partial T}{\partial r} \right)_{r=R} \quad (3.2)$$

In non-dimensional form,

$$Nu = -R \frac{k_{nf}}{k_f} \left( 1 + \frac{16\sigma^* T_\infty^3}{3k^*} \right) \frac{T_b - T_\infty}{R} \left( \frac{\partial T^*}{\partial r^*} \right)_{r^*=1} \quad (3.3)$$

Since

$$q_r = \frac{16\sigma^* T_\infty^3}{3k^*} \frac{\partial T}{\partial r} \quad (3.4)$$

equation (3.3) simplifies to

$$Nu = -\frac{k_{nf}}{k_f} (1 + q_r) \left( \frac{\partial T^*}{\partial r^*} \right) \quad (3.5)$$

Space discretization for Nusselt number given in equation (3.5) is done based on backward finite difference at  $r = 1$  to  $r = 0$ . Therefore, the Nusselt is written as

$$Nu = -\frac{k_{nf}}{k_f} (1 + q_{ri}) \left( \frac{T_j - T_{j-1}}{\Delta r} \right) \quad (3.6)$$

$q_{ri}$  is the heat flux at point  $i$ .

The Sherwood number is given by

$$Sh = \frac{Rq_m}{D_{nf}(C_b - C_\infty)} \quad (3.7)$$

where

$$q_m = D_{nf} \left( -\frac{\partial C}{\partial r} \right)_{r=R} \quad (3.8)$$

Sherwood can be further written as

$$\begin{aligned} Sh &= -D_{nf} \left( \frac{\partial C}{\partial r} \right) \frac{R}{D_{nf}(C_b - C_\infty)}_{r=R} \\ &= -\frac{\partial C^*}{\partial r^*}_{r^*=1} \end{aligned} \quad (3.9)$$

Similarly, backward finite difference for equation (3.9) is expressed as follows:

$$Sh = -\frac{C_j - C_{j-1}}{\Delta r} \quad (3.10)$$

It is a dimensionless parameter used to describe frictional resistance by a fluid on a solid surface as it flows over it. This quantity provides a measure of the resistance to the fluid caused by its flow and interaction with the surface. Skin friction coefficient is dependent on factors such as fluid properties, fluid flow velocity, viscosity, roughness or smoothness of the surface and diameter of the FBD. Skin friction coefficient is given by

$$C_f = \frac{R\tau_w}{U\mu_f} \quad (3.11)$$

where  $\tau_w$  is the wall shear stress and for newtonian fluid

$$\tau_w = \mu_{nf} \left. \frac{\partial v_z}{\partial r} \right|_{r=R} \quad (3.12)$$

Thus

$$C_f = \frac{R \mu_{nf} \partial v_z}{U \mu_f \partial r} \quad (3.13)$$

In dimensionless form

$$\begin{aligned} C_f &= \frac{\mu_{nf} \partial v_z^*}{\mu_f \partial r^*} \Big|_{r^*=1} \\ &= \frac{1}{(1-\phi)^{2.5}} \frac{\partial v_z}{\partial r} \end{aligned} \quad (3.14)$$

Using backward finite difference method, the skin friction is evaluated at  $r = 1$  and  $r = 0$  as follows

$$C_f = \frac{1}{(1-\phi)^{2.5}} \frac{U_j - U_{j-1}}{\Delta r} \quad (3.15)$$

#### 4. ENTROPY GENERATION

One of the major concerns for engineers and scientists is to adopt ways which can minimize energy waste in thermal systems. Energy losses causes disorder which is measured in form of energy. Entropy generation indicate wastage of useful energy and is an effective mechanism for identifying thermal inefficiencies in a system. Study of entropy generation is important in explaining the irreversibilities of thermal energy in FBD and needs to be minimized so as to improve its energy efficiency. Entropy generation provides ways which can be used to improve the design of thermal system such as FBD. Entropy generation is calculated from velocity, concentration and temperature profiles obtained from solution of momentum, mass and energy equations. In heat transfer analysis, equations (2.2), (2.3), (2.4) and (2.5). as expressed by Ullah et al. [14] and Riaz et al. [15] are mathematically used to express the reduction in energy losses as follows

$$\begin{aligned} S'_{gen} &= \underbrace{\frac{k_{nf}}{T_\infty^2} \left[ \left( 1 + \frac{16\sigma^*}{3k^*} T_\infty^3 \right) \left( \frac{\partial T}{\partial r} \right)^2 + \left( \frac{\partial T}{\partial z} \right)^2 \right]}_{1^{st}} + \underbrace{\frac{\mu_{nf}}{T_\infty} \left( \frac{\partial v_r}{\partial z} + \frac{\partial v_z}{\partial r} \right)^2}_{2^{nd}} + \\ &\underbrace{\frac{D_{nf}}{C_\infty} \left[ \left( \frac{\partial C}{\partial r} \right)^2 + \left( \frac{\partial C}{\partial z} \right)^2 \right]}_{3^{rd}} + \underbrace{\frac{D_{nf}}{T_\infty} \left( \frac{\partial C}{\partial r} \frac{\partial T}{\partial r} + \frac{\partial C}{\partial z} \frac{\partial T}{\partial z} \right) + \frac{\sigma_{nf} B_0^2}{T_\infty} V^2}_{4^{th}} \end{aligned} \quad (4.1)$$

Entropy generation in equation (4.1) is stated in four different parts. The first and second part is entropy generation due heat transfer and viscous dissipation irreversibility respectively. The third part is entropy generation due to diffusive irreversibility and lastly is entropy generation due the effects of magnetic field. The dimensionless form of entropy generation  $N_s$  is obtained by letting

$$N_s = \frac{S'_{gen}}{S''_{gen}} \quad (4.2)$$

where

$$S''_{gen} = \frac{k_f (T_b - T_\infty)^2}{R^2 T_\infty^2} \quad (4.3)$$

In non-dimensional form, volumetric rate of entropy generation is expressed as follows

$$\begin{aligned}
 N_s = \frac{k_{nf}}{k_f} \left[ \left( 1 + \frac{16\sigma^*}{3k^*} T_\infty^3 \right) \left( \frac{\partial T^*}{\partial r^*} \right)^2 + \left( \frac{\partial T^*}{\partial z^*} \right)^2 \right] + \frac{U^2 \mu_{nf} T_\infty}{k_f (T_b - T_\infty)^2} \left( \frac{\partial v_r^*}{\partial z^*} + \frac{\partial v_z^*}{\partial r^*} \right)^2 + \\
 \frac{D_{nf} T_\infty^2 (C_b - C_\infty)^2}{k_f C_\infty (T_b - T_\infty)^2} \left[ \left( \frac{\partial C^*}{\partial r^*} \right)^2 + \left( \frac{\partial C^*}{\partial z^*} \right)^2 \right] + \\
 \frac{D_{nf} T_\infty}{k_f} \frac{C_b - C_\infty}{T_b - T_\infty} \left( \frac{\partial C^*}{\partial r^*} \frac{\partial T^*}{\partial r^*} + \frac{\partial C^*}{\partial z^*} \frac{\partial T^*}{\partial z^*} \right) + \frac{\sigma_{nf} \mu_e^2 H_0^2 V^2 R^2 T_\infty}{k_f (T_b - T_\infty)^2}
 \end{aligned} \tag{4.4}$$

Expressing the above equation in terms of non-dimensional parameters, it can be simplified as follows:

$$\begin{aligned}
 N_s = \frac{k_{nf}}{k_f} \left[ \left( 1 + \frac{16\sigma^*}{3k^*} T_\infty^3 \right) \left( \frac{\partial T^*}{\partial r^*} \right)^2 + \left( \frac{\partial T^*}{\partial z^*} \right)^2 \right] + \frac{1}{(1-\phi)^{2.5}} \frac{EcPr}{\lambda_1} \left( \frac{\partial v_r^*}{\partial z^*} + \frac{\partial v_z^*}{\partial r^*} \right)^2 + \\
 \frac{\Gamma \lambda_2}{\lambda_1} \left[ \left( \frac{\partial C^*}{\partial r^*} \right)^2 + \left( \frac{\partial C^*}{\partial z^*} \right)^2 \right] + \Gamma \left( \frac{\partial C^*}{\partial r^*} \frac{\partial T^*}{\partial r^*} + \frac{\partial C^*}{\partial z^*} \frac{\partial T^*}{\partial z^*} \right) + \frac{\phi_8 Ec Pr M}{\lambda_1}
 \end{aligned} \tag{4.5}$$

where  $\phi_8 = (1 - \phi)\sigma_f + \phi\sigma_s$ ,  $\lambda_1$  and  $\lambda_2$  are parameters for temperature and concentration differences respectively while  $\Gamma$  gives a ratio of concentration to temperature differences. They are given by the following formulas

$$\Gamma = \frac{D_{nf} T_\infty}{k_{nf}} \left( \frac{C_b - C_\infty}{T_b - T_\infty} \right) \tag{4.6}$$

$$\lambda_1 = \frac{T_b - T_\infty}{T_\infty} \tag{4.7}$$

$$\lambda_2 = \frac{C_b - C_\infty}{C_\infty} \tag{4.8}$$

In finite difference form, equation of entropy generation is expressed as

$$\begin{aligned}
 N_s = \frac{k_{nf}}{k_f} \left[ \left( 1 + \frac{16\sigma^*}{3k^*} T_\infty^3 \right) \left( \frac{T_{j+1,k}^i - T_{j-1,k}^i}{2\Delta r} \right)^2 + \left( \frac{T_{j,k+1}^i - T_{j,k-1}^i}{2\Delta z} \right)^2 \right] + \\
 \frac{1}{(1-\phi)^{2.5}} \frac{EcPr}{\lambda_1} \left( \frac{U_{j,k+1}^i - U_{j,k-1}^i}{2\Delta z} + \frac{V_{j+1,k}^i - V_{j-1,k}^i}{2\Delta r} \right)^2 + \\
 \frac{\Gamma \lambda_2}{\lambda_1} \left[ \left( \frac{C_{j+1,k}^i - C_{j-1,k}^i}{2\Delta r} \right)^2 + \left( \frac{C_{j,k+1}^i - C_{j,k-1}^i}{2\Delta z} \right)^2 \right] + \\
 \Gamma \left( \left( \frac{C_{j+1,k}^i - C_{j-1,k}^i}{2\Delta r} \right) \left( \frac{T_{j+1,k}^i - T_{j-1,k}^i}{2\Delta r} \right) + \left( \frac{C_{j,k+1}^i - C_{j,k-1}^i}{2\Delta z} \right) \left( \frac{T_{j,k+1}^i - T_{j,k-1}^i}{2\Delta z} \right) \right) + \\
 \frac{\phi_8 Ec Pr M}{\lambda_1}
 \end{aligned} \tag{4.9}$$

The entropy generation number  $N_s$  can be represented as the sum of the entropy generated by thermal radiation  $N_1$ , viscous dissipation  $N_2$ , concentration diffusion  $N_3$  and magnetic field  $N_4$ . That is

$$N_s = N_1 + N_2 + N_3 + N_4 \quad (4.10)$$

## 5. BEJAN NUMBER

Bejan number (Be) is used to determine whether entropy generated by heat transfer is greater than that generated by viscous dissipation, concentration diffusion and magnetic field, or vice versa. It is defined as the ratio of entropy generated by heat transfer to the total entropy generation in FBD. Bejan number is important because it helps to identify which irreversibility mechanism is dominant in a system. If the Bejan number is large, then heat transfer irreversibilities are dominant and the system is said to be heat transfer controlled. On the other hand, if the Bejan number is small, then fluid flow irreversibilities are dominant and the system is said to be fluid flow controlled. By using the Bejan number, engineers and researchers can design systems that minimize entropy generation and improve overall system efficiency. They can also use the Bejan number to identify the source of irreversibilities in a system and develop strategies to reduce them. Be is given by

$$Be = \frac{N_1}{N_s} = \frac{1}{1 + \psi} \quad (5.1)$$

where  $\psi = \frac{N_2 + N_3 + N_4}{N_1}$  gives the ratio due to irreversibilities.

Bejan number Be varies between 0 and 1. A value of  $Be \rightarrow 1$  indicates that irreversibility due to heat transfer is dominant over the irreversibility due to fluid friction. Conversely, a value of  $Be \rightarrow 0$ , means that the fluid friction is more significant than irreversibility due to heat transfer. Moreover, a value of  $Be = \frac{1}{2}$  indicates irreversibilities due to heat transfer and fluid friction are of same magnitude.

## 6. RESULTS AND DISCUSSION

The Table below depicts how the Nusselt number ( $Nu$ ), Sherwood number ( $Sh$ ) and the Skin Friction Coefficient ( $Cf$ ) vary with various fluid flow parameters.

M	Pr	Ec	Re	Phi	qr	Grc	GrT	Sc	K	Nu	Sh	Cf
<b>2.0</b>	0.71	0.2	2	0.2	0.5	2	0.2	0.22	2	-0.0951	1.08810	-2.0251
<b>4.0</b>	0.71	0.2	2	0.2	0.5	2	0.2	0.22	2	-0.0953	1.08806	-2.0691
<b>6.0</b>	0.71	0.2	2	0.2	0.5	2	0.2	0.22	2	-0.0955	1.08812	-2.1137
<b>8.0</b>	0.71	0.2	2	0.2	0.5	2	0.2	0.22	2	-0.0982	1.10460	-2.5397
2.0	0.71	<b>0.25</b>	2	0.2	0.5	2	0.2	0.22	2	-0.1076	1.08786	-2.5063
2.0	0.71	<b>0.4</b>	2	0.2	0.5	2	0.2	0.22	2	-0.3064	2.72000	-0.5053
2.0	0.71	0.4	<b>2</b>	0.2	0.5	2	0.2	0.22	2	-0.0286	3.3600	-0.4581
2.0	0.71	0.4	<b>4</b>	0.2	0.5	2	0.2	0.22	2	-0.0181	3.5733	-0.4426
2	0.71	0.2	<b>6</b>	0.2	0.5	2	0.2	0.22	2	0.0311	3.6800	-0.4349
2	0.71	0.2	2	<b>0.2</b>	0.5	2	0.2	0.22	2	-0.0962	2.7213	-0.8868
2	0.71	0.2	2	<b>0.3</b>	0.5	2	0.2	0.22	2	-0.0975	2.7192	-0.7461
2	0.71	0.2	2	<b>0.4</b>	0.5	2	0.2	0.22	2	-0.2930	2.7185	-0.6094
2	0.71	0.2	2	0.2	<b>0.5</b>	2	0.2	0.22	2	-0.2615	1.1746	-0.5063
2	0.71	0.2	2	0.2	<b>1.0</b>	2	0.2	0.22	2	-0.2252	0.8721	-2.7020
2	0.71	0.2	2	0.2	0.5	<b>4</b>	0.2	0.22	2	-0.0618	0.8345	-1.8251
2	0.71	0.2	2	0.2	0.5	<b>6</b>	0.2	0.22	2	-0.0668	1.0881	-0.8691
2	0.71	0.2	2	0.2	0.5	2	<b>0.4</b>	0.22	2	-0.06181	1.1233	-2.1251
2	0.71	0.2	2	0.2	0.5	2	<b>0.6</b>	0.22	2	-0.0619	1.2312	-2.5251
2	0.71	0.2	2	0.2	0.5	2	0.2	<b>0.23</b>	2	-1.9801	1.9487	-0.3906
2	0.71	0.2	2	0.2	0.5	2	0.2	<b>0.24</b>	2	-3.5904	6.1631	-0.9479
2	0.71	0.2	2	0.2	0.5	2	0.2	0.22	<b>3</b>	-1.5504	1.7622	-0.0593
2	0.71	0.2	2	0.2	0.5	2	0.2	0.22	<b>4</b>	-3.0817	7.4487	-4.1740

TABLE 1. Variation of Coefficients of friction, Sherwood and Nusselt numbers with various parameters.

Table 1 shows the effects of magnetic parameter, Eckert number, Reynolds number, nanoparticle volume fraction coefficient, heat and mass transfer Grashof number, Schmidt number and chemical reaction parameter on Nusselt number, Sherwood number and skin friction coefficient.

Increase in Hartmann number (M) led to an increase in Sherwood number (Sh) and decrease in both Nusselt number (Nu) and Skin friction coefficient (Sh). Increase in magnetic field strength signifies stronger Lorentz forces which retards the motion of the fluid flow within the dryer. This inhibits convective heat transfer hence the decrease in Nusselt number. Also, increased magnetic field strength results in thinner concentration boundary layer which means that the concentration gradient is greater. Higher concentration gradient enhances mass transfer hence increase in Sherwood number. Moreover, stronger magnetic field strength reduces the fluid's

velocity due to presence of Lorentz force which opposes the flow. The decrease in fluid flow velocity results in decreased frictional forces and shear stresses hence reduced skin friction coefficient.

Increase in Eckert number ( $Ec$ ) results in increase in Sherwood number and skin friction coefficient but a decrease in Nusselt number. High Eckert number implies high kinetic energy in the flow compared to thermal energy. Increased kinetic energy increases the fluid's velocity which reduces the convective heat transfer. This then leads to reduced Nusselt number. Moreover, increased Sherwood number as Eckert is increased means more efficient and improved convective mass transfer. Increase in Eckert number leads to a thinner boundary layer near the dryer's surface. Thinner boundary layer enhances mass transfer rate hence increased Sherwood number.

As Reynolds number increases Nusselt number, Sherwood number and skin friction coefficient also increases. High Reynolds number indicates increased fluid flow velocity. High velocity leads to increase in convective heat transfer rate and mass transfer rates which raises the Nusselt number and Sherwood number respectively. High Reynolds number denotes dominance of inertial forces which results in high fluid flow velocity. Increase in Reynolds number increases the thickness of the surface boundary layer. This creates more contact between the fluid and the dryer's surface hence increased skin friction coefficient.

Increase in nanoparticle volume fraction led to decrease in Nusselt number and Sherwood number. The silver nanoparticles have high thermal conductivity. When added to fluid in the dryer, it increases the thermal conductivity hence affecting the convective heat transfer which result in decrease in Nusselt number. Moreover, increase in fluid's viscosity as a result of increased nanoparticle volume fraction hampers the mass transfer rate which in turn reduces the Sherwood number. However, increase in nanoparticles lead to increased skin friction coefficient. Increase of nanoparticle volume fraction raises the fluid's viscosity resulting in high frictional resistance. This effect leads to increased skin friction coefficient.

Increase in radiation parameter led to increase in Nusselt number and skin friction coefficient but a decrease in Sherwood number. Nusselt number represents the ratio of convective heat transfer to conductive heat transfer. An increase in radiation parameter signifies an increase in radiative heat transfer relative to conductive heat transfer. This thus enhances the overall heat transfer rate in the dryer leading to higher Nusselt number. The Skin friction coefficient is associated with drag force experienced by a fluid moving over a surface. Increase in radiation parameter alters temperature distribution on the dryer's surface which in turn affects fluid's velocity and flow pattern. These changes thus affect the skin friction coefficient. Increased radiation affects the concentration distribution of species in the fluid. It reduces concentration gradient which lowers convective mass transfer rates compared to diffusive mass transfer rates. This then leads to a decrease in Sherwood number.

As concentration Grashof number increased, Nusselt number decreased while both Sherwood number and Skin friction coefficient increased. Increase in concentration Grashof number indicates that the buoyancy driven mass transfer due to concentration gradient is significant in the fluid flow.

Stronger buoyancy driven flow caused by concentration differences result in thinner boundary layer and reduced convective heat transfer. This then leads to decrease in Nusselt number. On the other hand, increase in concentration Grashof number indicates high convective mass transfer which corresponds to increase in Sherwood number. This indicates more efficient mass transfer within the dryer. Skin friction coefficient is associated with shear stress which measures frictional forces between the fluid and the surface. Thus an increase in shear stress caused by stronger buoyancy driven flow as a result of high concentration Grashof number leads to increase in skin friction coefficient.

Increase in local thermal Grashof number lead to increase in Sherwood number but a decrease in Nusselt number and skin friction coefficient. Increase in thermal Grashof number indicates stronger buoyancy driven natural convection flow due to larger temperature differences rather than viscous forces. Increased buoyancy forces leads to increased fluid velocity. Increase in fluid's velocity leads to thinner boundary layer within the dryer's surface where mass transfer occurs hence increase in Sherwood number. Enhanced natural convection decreases thickness of boundary layer due to increased fluid's motion within the dryer's surface thus reducing the convective heat transfer. This results in decrease in Nusselt number. Moreover, thinner boundary layers lead to decreased shear stress within the dryer's surface. This means that there is decreased fluid contact with the surface which exerts frictional forces. This contributes to decrease in skin friction coefficient.

Increasing Schmidt number results in decrease in Nusselt number and Skin friction coefficient with an increase in Sherwood number. Schmidt number is the ratio of momentum diffusivity to mass diffusivity. It represents the relative importance of momentum to mass transport. High Schmidt number indicates that the fluid has reduced ability to transport mass. Limited mass transfer lead to reduced fluidization and lower convective heat transfer which results in lower Nusselt number. Increase in Schmidt number decreases the concentration boundary layer thickness which reduces velocity gradient within the dryer. This consequently decreases the skin friction coefficient. Sherwood number represents ratio of convective to diffusive mass transfer. When both convective and molecular diffusion contribute to overall mass transfer rate, convective mass transfer becomes more dominant due to inefficient mass diffusion associated with higher Schmidt number. This thus leads to increase in Sherwood number.

It is also observed that increase in chemical reaction parameter increased Sherwood number but led to a decrease in Nusselt number and skin friction coefficient. Increase in chemical reaction parameter indicates enhanced reaction rates which enhances mass transfer within the dryer. As a result, the Sherwood number increases. Reduction in Nusselt number as chemical reaction parameter increases is attributed to cooling of the fluid within the dryer's surface. This reduces the temperature gradient which decreases the buoyancy driven convection flow leading to lower Nusselt number. Increase in chemical reaction parameter is associated with increased fluid's motion and momentum transfer within the boundary layer. This disrupts formation of boundary

layer and as a result leads to reduction of shear stress at the dryer's wall. This then lowers the skin friction coefficient.

### EFFECTS OF FLUID FLOW PARAMETERS ON ENTROPY GENERATION

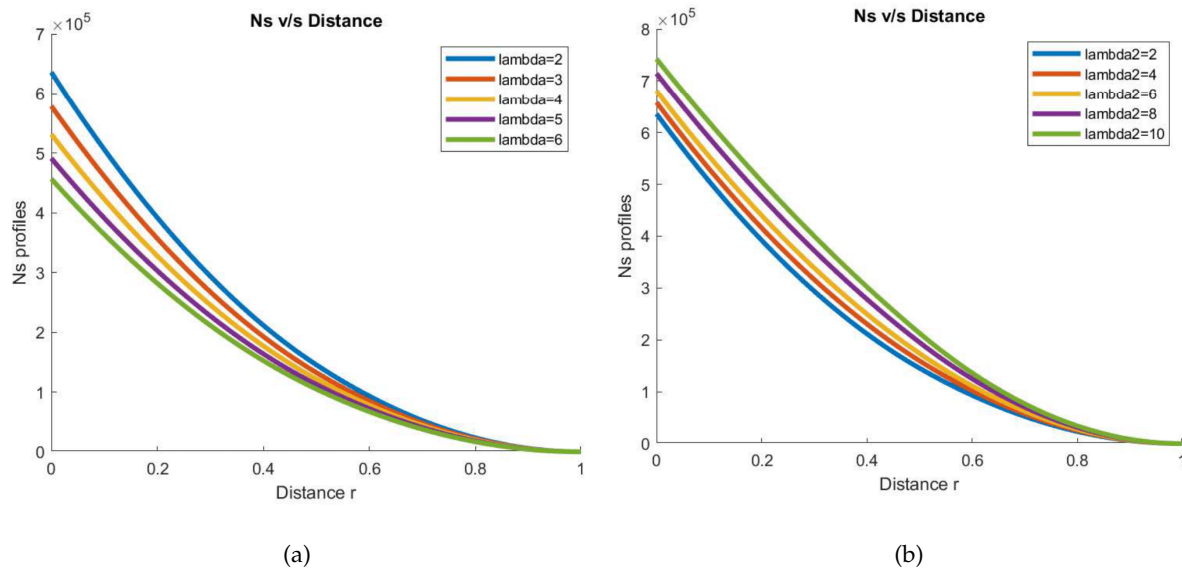


FIGURE 2. Influence of Temperature and Concentration ratio parameter on Entropy Generation

The effect of temperature difference parameter  $\lambda_1$  on entropy generation is displayed in figure 2a. From the second law of thermodynamics, heat flows naturally from higher to lower temperature regions. When temperature difference between two regions in the dryer increases, heat transfer also increases leading to higher thermal efficiency. Consequently, improved efficiency or reduction in energy losses result in low entropy production. Figure 2b depicts the effect of concentration ratio parameter on entropy generation. An increase in concentration ratio parameter  $\lambda_2$  raises entropy production. An increase in concentration ratio parameter shows a difference in concentration between two regions of the dryer. The concentration difference causes diffusion where particles move from higher to lower concentration regions. The movements of particles within the dryer cause a disorder within the dryer leading to an increase in entropy generation.

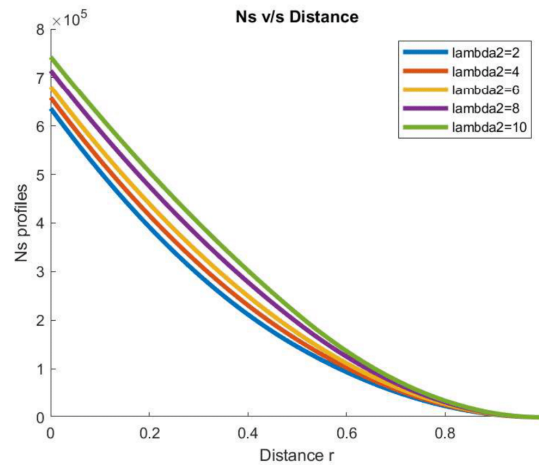


FIGURE 3. Effects of Hartmann number on Entropy Generation

It is observed from figure 3 that Entropy production decreases for increasing values of Hartmann number. Increase in Hartmann number signifies stronger magnetic forces compared to viscous forces in the flow. Increase in Hartman number suppresses the motion of the fluid perpendicular to the magnetic fields. When the fluid’s motion is suppressed, it reduces the velocity gradients in the fluid lowering the viscous dissipation. Viscous dissipation describes irreversible process where work is transformed by fluid on adjacent layers as a result of shear forces into thermal energy. Reduction in viscous dissipation therefore, is a source of energy loss which contributes to entropy production. The minimization of fluid friction and energy losses leads to reduction of entropy production.

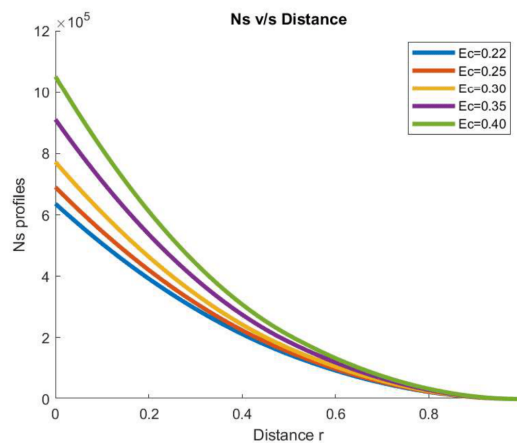


FIGURE 4. Effects of Eckert number on Entropy Generation

Figure 4 demonstrates the impact of Eckert number ( $Ec$ ) on entropy generation. As  $Ec$  increases, entropy generation is enhanced. This means that as the value of the Eckert number rises, the entropy production within the system intensifies. Viscous dissipation results from the friction between fluid layers moving at different velocities and it converts mechanical energy into thermal energy. As the Eckert number increases, the kinetic energy of the flow becomes more dominant relative to the thermal energy. Consequently, the viscous forces become stronger, causing more resistance to flow, and leading to an increase in entropy generation. This aligns with the physical observation that a higher  $Ec$  value strengthens the viscous force, increasing flow resistance and consequently, causing more entropy production.

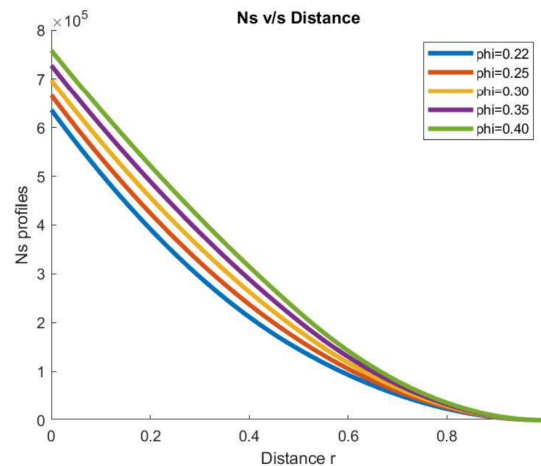


FIGURE 5. Effects of Nanoparticle volume fraction on Entropy Generation

Increase in nanoparticle volume fraction led to an increase in entropy production as observed in figure 5. Silver nanoparticles are good thermal conductors and can alter the thermal conductivity of the fluid. This leads to changes in heat transfer potentially causing temperature gradients within the flow. This raises entropy production since heat is transferred along the gradients. Also, increase in nanoparticle volume fraction increases the fluid's viscosity. Viscosity is measure of a fluid's resistance to flow. When fluid flows, it experiences internal friction which causes lose of kinetic energy, which in turn is converted to thermal energy. According to second law of thermodynamics, any irreversible process leads to increase in entropy hence the conversion of kinetic energy to thermal energy results in increased entropy production.

#### EFFECTS OF FLUID FLOW PARAMETERS ON BEJAN NUMBER

Investigating Bejan number serves the purpose of understanding the balance between heat transfer entropy generation and other factors such as magnetic field, fluid friction and thermal radiation entropy generation. Bejan number gives insights on the dominant mechanisms which govern the heat transfer and fluid flow in a fluidized bed dryer.

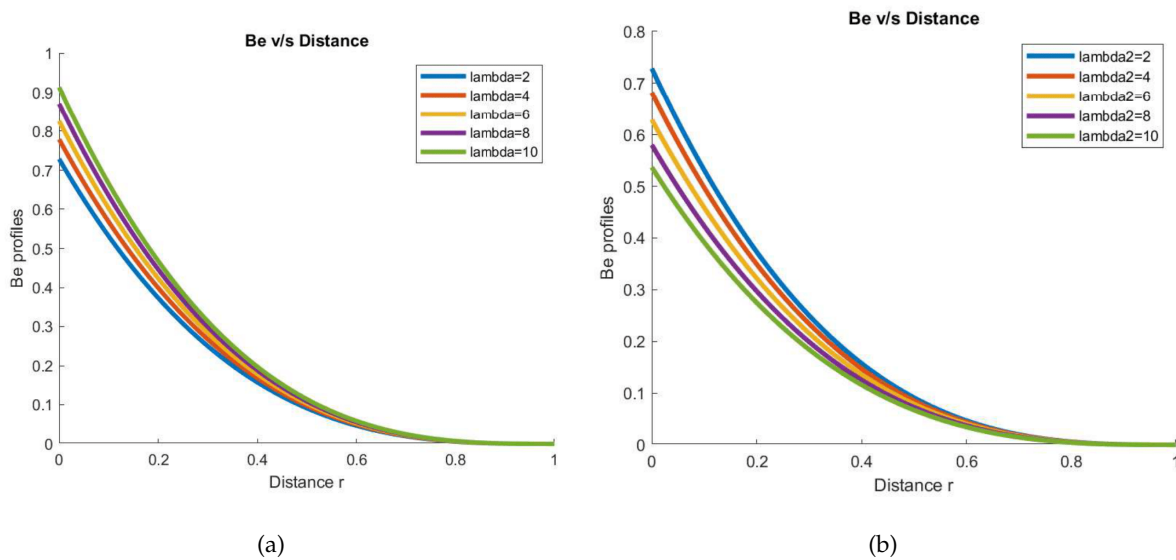


FIGURE 6. Influence of Temperature and Concentration ratio parameter on Bejan number

Enhancing the temperature ratio parameter  $\lambda_1$  increases the Bejan number  $Be$  as presented in figure 6a. Increase in temperature ratio indicates larger temperature differences between regions within the dryer. Larger temperature differences results in high transfer rates which can lead to increased thermal losses. This then contributes to overall irreversibility related to heat transfer hence increase in Bejan number. This indicates that irreversibilities in the dryer is majorly contributed by heat transfer inefficiencies and thus thermal irreversibility dominates over other irreversibilities. The concentration ratio parameter  $\lambda_2$  relates to the concentration difference within the dryer between different regions. Increase in concentration ratio parameter indicates larger concentration differences between regions in the dryer. Concentration gradients drive mass transfer processes from higher to lower concentration regions. As concentration parameter increases, concentration gradient becomes more evident hence increase in mass transfer and subsequently leading to irreversibilities related to mass transfer. This leads to decreased Bejan number as depicted in figure 6b. This indicates that mass transfer related inefficiencies contribute to the dryers' irreversibilities compared to heat transfer processes.

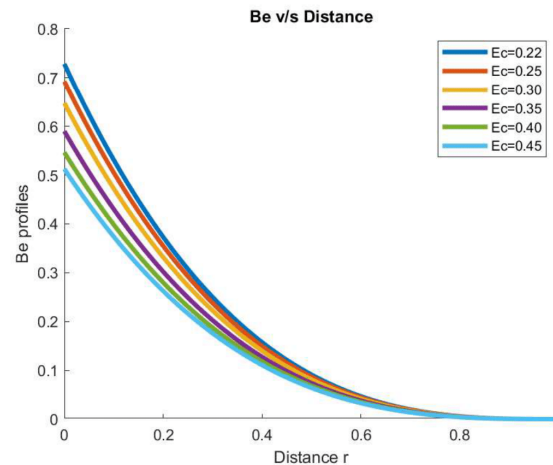


FIGURE 7. Effects of Eckert number on Bejan number

Figure 7 illustrates the effects of Eckert number  $Ec$  on the Bejan number  $Be$  for nanofluid flow. Eckert number quantifies the ratio of kinetic energy to heat transfer in the fluid flow while Bejan number gives the ratio of irreversibility due to heat transfer to total irreversibilities in the dryer. Increase in  $Ec$  indicates kinetic energy change in the fluid flow is more significant compared to heat transfer. This is due to increased kinetic energy of the nanofluid flow within the dryer, indicating greater manifestation of irreversibility due to fluid friction. Therefore, Eckert number  $Ec$ , gives a more pronounced effects of fluid motion relative to heat transfer which subsequently contributes to irreversibility to fluid friction compared to the total irreversibility hence raising the Bejan number.

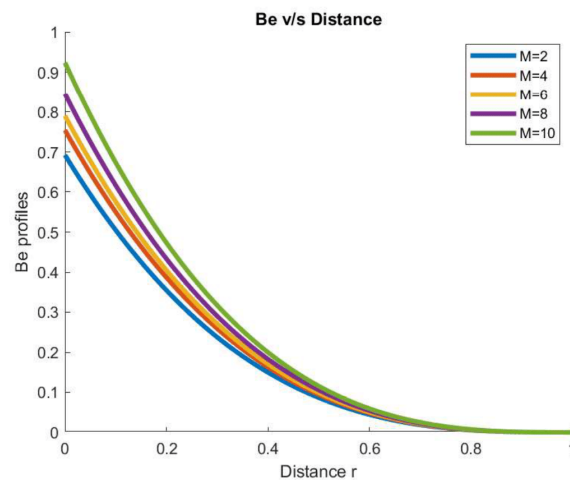


FIGURE 8. Effects of Hartmann number on Bejan number

Figure 8 illustrates the effects of Hartmann number  $M$  on the Bejan number  $Be$ . Hartmann number gives the relative strength of magnetic forces to viscous forces in the fluid flow within the dryer. Increase in Hartmann number signifies substantial influence of magnetic field strength compared to viscous effects within the fluid. When increase in Hartmann number leads to an increase in Bejan number, it indicates relative importance of viscous dissipation as source of entropy production compared to heat transfer.

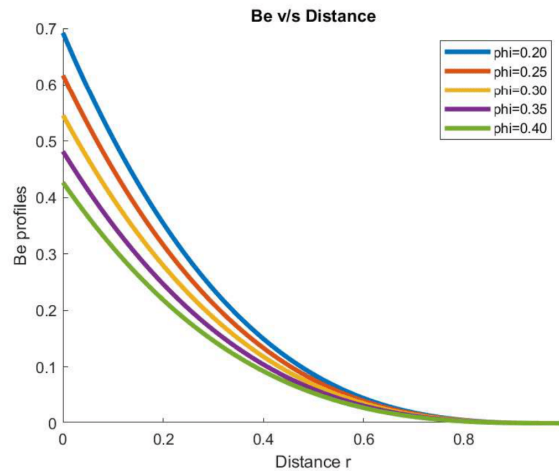


FIGURE 9. Effects of Nanoparticle volume fraction on Bejan number

It is seen from figure 9 that Bejan number increases with increase in nanoparticle volume fraction  $\phi$ . Increasing nanoparticle volume fraction affects the fluid's heat transfer characteristics. Nanoparticles have high thermal conductivity compared to the base fluid and when dispersed in the fluid they increase the overall thermal conductivity of the nanofluid. Increase in Bejan number can be attributed to high thermal conductivity associated with silver nanoparticles. This enhances the overall heat transfer in the dryer. The increase in heat transfer leads to a more pronounced heat transfer related irreversibilities leading to increased Bejan number.

## 7. VALIDATION

The results of our study were compared with those of Inaba et al. [7] who conducted comprehensive investigation into efficiency of fluidized bed dryer by developing exergy models with the aim of predicting drying efficiency. Although our model considered nanoparticle enhanced and magnetic field assisted drying conditions, there was significant agreement with findings of our study. This highlights our findings as practical and could improve the way various materials are dried in fluidized beds. Comparison was also made between the findings of this study and those of Motevali et al. [16] who acknowledged the significance of energy efficiency as primary criteria for assessing the dryers used in tea processing industries. According to their findings, low

entropy production in drying process was attributed to faster air flows and higher temperatures. This highlights our findings as practical and could improve the way various materials are dried in fluidized beds.

## 8. CONCLUSION

Entropy generation distribution due to heat and mass transfer in a fluidized bed dryer used in tea processing industry has been studied. By taking into account the variable magnetic field and nanoparticles, expressions for entropy generation and Bejan number are obtained and presented in plots. Results for skin friction coefficient, heat and mass transfer are computed in tabular form. The following conclusions are drawn from this work.

- The parameters  $M$ ,  $Ec$ ,  $GrT$ ,  $GrC$ ,  $Sc$  enhanced the rate of mass transfer but had an opposing effect on the rate of heat transfer.
- The parameters  $Re$  and  $q$  increased the skin friction coefficient and the Nusselt number.
- Addition of nanoparticles in the fluid flow within the dryer improved the rate of mass transfer and the skin friction coefficient but decreased the Nusselt number.
- The Sherwood number and skin friction coefficient increased with rise in  $Re$  and  $Ec$ ,  $GrC$  while it decreased with increase in radiation parameter and  $M$ ,  $GrT$ ,  $Sc$ ,  $K$  respectively.
- The parameters  $Re$  and  $q$  decreases the rate of heat transfer while  $M$ ,  $Ec$ ,  $GrT$ ,  $GrC$ ,  $Sc$ ,  $K$  and  $\phi$  tend to increase its effect. On the other hand, the rate of mass transfer is enhanced with increasing values of  $M$ ,  $EC$ ,  $Grt$ ,  $Grc$ ,  $Sc$ ,  $K$  and  $Re$  while  $\phi$  and  $q$  have a negative effect on it. The skin friction coefficient gets increased with increased values of  $Ec$ ,  $Re$ ,  $q$ ,  $GrC$  and  $\phi$  however  $M$ ,  $Grt$ ,  $Sc$  and  $K$  have an opposing impact on it.
- Entropy generation increases with increase in concentration difference however it has opposing effect on Bejan number.
- Entropy generation reduces with increased temperature within the dryer and increased magnetic field strength however the opposite observation is made on Bejan number which increases for increasing values of temperature and magnetic field strength.
- Entropy generation and Bejan number increases for increased values of Eckert number and nanoparticle volume fraction.

**Acknowledgment.** The authors would like to express their appreciation to the African Union Commission and the Pan African University, Institute for Basic Sciences, Technology, and Innovation for their steadfast support in conducting this research.

**Conflicts of Interest:** The authors declare that there are no conflicts of interest regarding the publication of this paper.

## REFERENCES

- [1] R. Clausius, *The Mechanical Theory of Heat*, Macmillan, London, 1879.

- [2] A. Bejan, A Study of Entropy Generation in Fundamental Convective Heat Transfer, *J. Heat Transfer*. 101 (1979), 718–725. <https://doi.org/10.1115/1.3451063>.
- [3] A. Bejan, Second-Law Analysis in Heat Transfer and Thermal Design, *Adv. Heat Transfer*. 15 (1982), 1–58. [https://doi.org/10.1016/s0065-2717\(08\)70172-2](https://doi.org/10.1016/s0065-2717(08)70172-2).
- [4] A. Bejan, The thermodynamic design of heat and mass transfer processes and devices, *Int. J. Heat Fluid Flow*. 8 (1987), 258–276. [https://doi.org/10.1016/0142-727x\(87\)90062-2](https://doi.org/10.1016/0142-727x(87)90062-2).
- [5] A. Bejan, Method of entropy generation minimization, or modeling and optimization based on combined heat transfer and thermodynamics, *Rev. Gén. Therm.* 35 (1996), 637–646. [https://doi.org/10.1016/s0035-3159\(96\)80059-6](https://doi.org/10.1016/s0035-3159(96)80059-6).
- [6] V. Bulgakov, I. Sevostianov, G. Kaletnik, I. Babyn, S. Ivanovs, I. Holovach, Y. Ihnatiev, Theoretical Studies of the Vibration Process of the Dryer for Waste of Food, *Rural Sustain. Res.* 44 (2020), 32–45. <https://doi.org/10.2478/plua-2020-0015>.
- [7] H. Inaba, H. Syahrul, A. Horibe, N. Haruki, Heat and Mass Transfer Analysis of Fluidized Bed Grain Drying, *Mem. Fac. Eng. Okayama Univ.* 41 (2007), 52–62. <https://doi.org/10.18926/14084>.
- [8] M. Deymi-Dashtebayaz, A. Arabkoohsar, F. Darabian, Energy and Exergy Analysis of Fluidised Bed Citric Acid Dryers, *Int. J. Exergy*. 22 (2017), 218–234. <https://doi.org/10.1504/ijex.2017.083169>.
- [9] S. A. H. Razavikia, H. amirzade, V.Ehterami, R. moeinzadeh, E. kianfar, Modeling Thermodynamic Drying Bed Fluid, *MEANJIN - Arts Human. J.* 7 (2015), 163–172.
- [10] S.U. Choi, J.A. Eastman, Enhancing Thermal Conductivity of Fluids With Nanoparticles, *Tech. Rep.*, Argonne National Lab. (ANL), Argonne, IL, United States, (1995).
- [11] A. El Jery, N. Hidouri, M. Magherbi, A.B. Brahim, Effect of an External Oriented Magnetic Field on Entropy Generation in Natural Convection, *Entropy*. 12 (2010), 1391–1417. <https://doi.org/10.3390/e12061391>.
- [12] S. Das, R.N. Jana, Natural Convective Magneto-Nanofluid Flow and Radiative Heat Transfer Past a Moving Vertical Plate, *Alexandria Eng. J.* 54 (2015), 55–64. <https://doi.org/10.1016/j.aej.2015.01.001>.
- [13] R. Mehta, V.S. Chouhan, T. Mehta, Mhd Flow of Nanofluids in the Presence of Porous Media, Radiation and Heat Generation Through a Vertical Channel, *J. Phys.: Conf. Ser.* 1504 (2020), 012008. <https://doi.org/10.1088/1742-6596/1504/1/012008>.
- [14] H. Ullah, T. Hayat, S. Ahmad, M.S. Alhodaly, Entropy Generation and Heat Transfer Analysis in Power-Law Fluid Flow: Finite Difference Method, *Int. Commun. Heat Mass Transfer*. 122 (2021), 105111. <https://doi.org/10.1016/j.icheatmasstransfer.2021.105111>.
- [15] A. Riaz, A. Zeeshan, M.M. Bhatti, Entropy Analysis on a Three-Dimensional Wavy Flow of Eyring-Powell Nanofluid: A Comparative Study, *Math. Probl. Eng.* 2021 (2021), 6672158. <https://doi.org/10.1155/2021/6672158>.
- [16] A. Motevali, R. Amiri Chayjan, Effect of Various Drying Bed on Thermodynamic Characteristics, *Case Stud. Thermal Eng.* 10 (2017), 399–406. <https://doi.org/10.1016/j.csite.2017.09.007>.